ELSEVIER

Physica D 96 (1996) 30–46

PHYSICA D

Phase turbulence in the two-dimensional complex Ginzburg–Landau equation

Paul Manneville [a,b,*], Hugues Chaté [b,a]

[a] LadHyX – Laboratoire d'Hydrodynamique, Ecole Polytechnique, 91128 Palaiseau, France

[b] CEA – Service de Physique de l'Etat Condensé, Centre d'Etudes de Saclay, 91191 Gif-sur-Yvette, France

Abstract

Turbulence arising from the phase instability of planewaves in the complex Ginzburg–Landau equation is studied by means of numerical simulations of two-dimensional domains of linear size L ranging from 80 to 5120. It is shown that, although phase turbulence can be considered as sustained and statistically stationary in a finite region of parameter space for systems of finite size studied over a limited time period, it is likely to break down towards amplitude turbulence at the infinite-size infinite-time "thermodynamic limit." As long as it persists, however, the statistical properties of phase turbulence are well described within the framework of fluctuating interfaces. Parameters of an effective Kardar–Parisi–Zhang equation governing the large-scale phase fluctuations are evaluated. The logarithmic behavior predicted for the linear regime in two dimensions is observed. The crossover to the nontrivial scaling regime is estimated to take place at L several orders of magnitude larger than the largest size considered here.

1. Introduction

The study of chaos in spatially-extended systems close to an instability point rests mostly on universal approaches cast in terms of modulations of ideal patterns. Generically, these modulations are governed by envelope equations, the structure of which is determined by the symmetries of the problem [1]. The prototype of such envelope equations is the complex Ginzburg–Landau (CGL) equation [3]:

$$\partial_t A = A + (1 + \mathrm{i}c_1)\nabla^2 A - (1 - \mathrm{i}c_3)|A|^2 A\,, \qquad (1)$$

where $A = R\exp\mathrm{i}\phi$ is a complex field and c_1, c_3 the two remaining real parameters left after suitable rescaling. Accounting for the spatial unfolding of a Hopf bifurcation in a continuous medium, this equation is more specifically relevant to uniform oscillatory instabilities [5], but other cases, such as stationary cellular patterns or waves, can be similarly described [1,6].

The solutions of the CGL equation display a very rich spectrum of dynamical behavior when its parameters are varied, reflecting the interplay of dissipation, dispersion, and nonlinearity. In particular, complex disordered regimes have been observed. Numerical studies of the dynamical regimes of the CGL equation have produced "phase diagrams", in space dimensions $d = 1$ [7–9] and $d = 2$ [10–12]. Several types of spatio-temporally chaotic regimes, distinguished essentially by the presence/absence of "defects" (i.e., zeros of the

* Corresponding author.

PII S0167-2789(96)00045-0

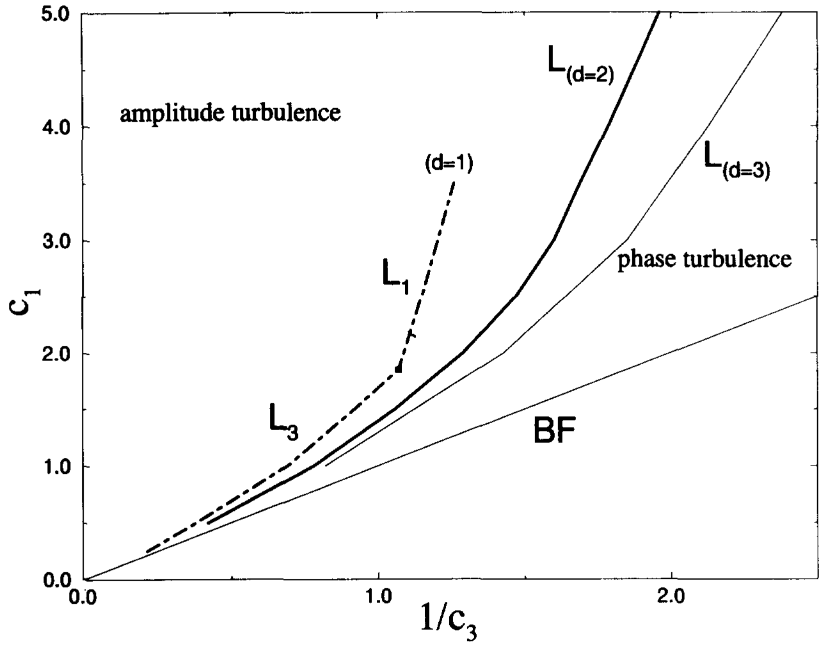

Fig. 1. Domain of observability of phase turbulence in the parameter plane for $d = 1, 2$ and 3. Results obtained by numerical simulations of systems of linear size L of the order 10^3 for $d = 1$ and 2. Results for the three-dimensional case, obtained on a system of size $L = 48$, are preliminary. The experimental protocol used consisted in approaching breakdown by varying slowly c_3, and, at each value considered, running the system during a fixed time of the order of $T = 5000$.

complex field A) have been observed. Whereas the disordered regimes with defects are called "defect-mediated turbulence" [13], "defect turbulence", or "amplitude turbulence" [7], phase turbulence is the term usually employed to describe those spatio-temporally chaotic regimes without defects. In fact, phase turbulence was one of the main subjects of the important early work of Kuramoto [14].

Fig. 1 shows the domain of the (c_1, c_3) plane where phase turbulence arising from a spatially uniform solution ("zero winding number") has been observed, as determined by numerical experiments following a well-defined systematic methodology. As will be recalled in Section 2, phase turbulence can be seen as the result of the phase instability of a family of regular planewave solutions which takes place for $1 - c_1c_3 < 0$ (Benjamin–Feir line "BF", see below). As the space dimension increases, the domain of observability of phase turbulence shrinks.

For $d = 1$, it is limited by two lines, initially called "L_1" and "L_3" [7]. Line L_1 is a continuous transition to amplitude turbulence which was later interpreted to correspond to a smooth crossover from a regime with a vanishingly small density of defects towards one characterized by a finite density of defects [15]. In this region, phase turbulence is the only "attractor". Line L_3, on the other hand, is the locus of a discontinuous transition: when a strong-enough local perturbation is nucleated, the amplitude turbulence regime invades phase turbulence quasi-deterministically [8,9]. Near L_3, phase turbulence is metastable and coexists with amplitude turbulence.

For $d = 2$, phase turbulence is observed between the BF line and a line called "L" in [12] beyond which, similarly to line L_3 in one space dimension, the nucleation of defects leads to the quasi-deterministic invasion by amplitude turbulence. In the two-dimensional case, phase turbulence is always metastable, and coexists with either or both amplitude turbulence and frozen, spatially-disordered cellular structures with defects [12].

In Section 2, we recall the issues surrounding the problem of *phase dynamics* before turning to the core of this paper: the statistical study of phase turbulence in the CGL equation itself. This study is divided in two parts. In Section 3, we treat the problem, left unresolved by the numerical works mentioned above, of the existence of phase turbulence in the infinite-size, infinite-time limit. In Section 4, we discuss the extent to which the long wavelength fluctuations can be described within a Langevin-like framework where chaos at small scales plays the role of a "microscopic" noise. This leads us to a better-known field of statistical physics from where we can infer the actual large-scale properties of phase turbulence. Our results are summarized and commented on in Section 5.

2. Phase dynamics for the CGL equation

Looking further for universal features, low-frequency, long-wavelength properties of envelope equations such as those mentioned in the introduction are of primary interest. These properties are tightly connected to those of the neutral modes associated with the continuous invariances of the medium undergoing the instability. For general reasons, translation invariance is linked to a *phase mode* [16], here a mode involving the phase ϕ of the complex amplitude $A = R\exp(\mathrm{i}\phi)$. More precisely, the relevant slow variable is the phase gradient $\nabla\phi$. Fast variables, e.g., fluctuations of the magnitude R, can be "adiabatically" eliminated, yielding at lowest order in $\nabla\phi$ an effective *phase equation*.

For the CGL equation, this procedure involves the study of "reference" regular planewave solutions which read:

$$A(\mathbf{x}, t) = R_q \exp[\mathrm{i}(\mathbf{q}\cdot\mathbf{x} - \omega_q t)]\,, \tag{2}$$

where R_q and ω_q can easily be obtained by substitution in (1):

$$R_q = \sqrt{1-q^2}, \qquad \omega_q = -c_3 + (c_1 + c_3)q^2,$$
$$q = |\mathbf{q}|. \tag{3}$$

The stability criterion of these solutions, derived from a standard stability analysis, involves the value of the underlying wavevector $\mathbf{q}$ and, of course, parameters c_1 and c_3. The least unstable wavevector is $\mathbf{q} = \mathbf{0}$, i.e., the solution corresponding to a spatially-uniform rotation with frequency $\omega_0 = -c_3$. The dynamics of perturbations around this solution can be obtained by a standard center manifold reduction which yields a set of equations governing the magnitude R and phase perturbations. At fourth-order in $\nabla\phi$, the phase dynamics obeys:

$$\begin{aligned}\partial_t\psi = {} & D\nabla^2\psi - K\nabla^4\psi + g_0(\nabla\psi)^2\\ & + g_1(\nabla\psi)(\nabla^3\psi) + g_2(\nabla^2\psi)^2\\ & + g_3(\nabla\psi)^2(\nabla^2\psi),\end{aligned} \tag{4}$$

with

$$\begin{aligned}&D = 1 - c_1c_3, \qquad K = \tfrac{1}{2}c_1^2(1+c_3^2),\\ &g_0 = -(c_1+c_3),\\ &g_1 = 2g_2 = c_1g_3 = -2c_1(1+c_3^2),\end{aligned} \tag{5}$$

where $\psi(\mathbf{x}, t)$ is the effective phase field parameterizing the manifold, i.e., a nonlinear transform of the original phase field ϕ (for a detailed derivation see, e.g., [17]).

When the phase diffusion coefficient $D = 1 - c_1c_3$ is positive, small phase perturbations relax, and it is legitimate to keep only the diffusion term in (4). On the other hand, when $D < 0$ (Newell's criterion), a *phase instability* – the so-called Benjamin–Feir instability [18] – occurs, and one has to take higher orders into account. Assuming $|D|$ small, a consistent truncation at order $|D|^3$ with $\partial_t\psi \sim \nabla^2\psi \sim |\nabla\psi|^2 \sim D\nabla^2\psi \sim |D|^3$ – which implies a length (time) scale diverging as $|D|^{-1/2}$ $\left(|D|^{-2}\right)$ as D approaches zero – yields the Kuramoto–Sivashinsky (KS) equation [19]:

$$\partial_t\psi = D\nabla^2\psi - K\nabla^4\psi + g_0\,(\nabla\psi)^2\,. \tag{6}$$

The KS equation is one of the major components of our understanding of space–time chaos [6]. It is well known for exhibiting bounded chaotic solutions for large-enough system sizes. The term "phase turbulence" [14,20], is often used to describe them, because the KS equation, in this context, governs a phase variable. However, it should be clear that, with respect to the CGL equation, the KS equation is a valid phase description only in the immediate vicinity of the BF line.

As a matter of fact, while the KS equation is mathematically well-behaved [21], this does not seem to be the case of the higher-order truncations of the phase dynamics such as Eq. (4). Indeed, finite-time singularities have been observed in numerical simulations [22,20]. Ongoing work aims at a systematic exploration of this situation in the relevant region of the (c_1, c_3) plane and for various orders of truncation of the phase gradient expansion leading to the phase equation.

The breakdown of the phase regime, marked by the (local) divergence of the phase gradient, is associated with the advent of a defect, i.e., a zero of A, in the CGL context. In practice, however, no firm conclusion about the breakdown of phase turbulence in the CGL equation itself can be drawn from the truncation of the phase gradient expansion at a finite order; one thus has to resort to direct simulations of the primitive equation to decide whether phase turbulence can be observed at finite distance from the BF line.

3. Existence of phase turbulence for CGL in two dimensions

The finite character of numerical experiments obviously leaves unanswered the theoretical question of the persistence of phase turbulence at the infinite-time infinite-size limit. As usual in statistical mechanics, one can nevertheless provide an educated guess by extrapolating carefully-studied finite-size and finite-time effects.

Before presenting our results, we recall some of the basic phenomenology of the phase turbulence regimes of CGL. One of the striking features is the presence of cellular structures (Fig. 2). Their origin is easily understood in the context of the phase Eq. (4) introduced in Section 2. Linear stability analysis immediately leads to the existence of a most-unstable wavelength:

$$\lambda_{\max} = 2\pi\sqrt{\frac{2K}{|D|}} \sim |1 - c_1 c_3|^{-1/2}\,, \qquad (7)$$

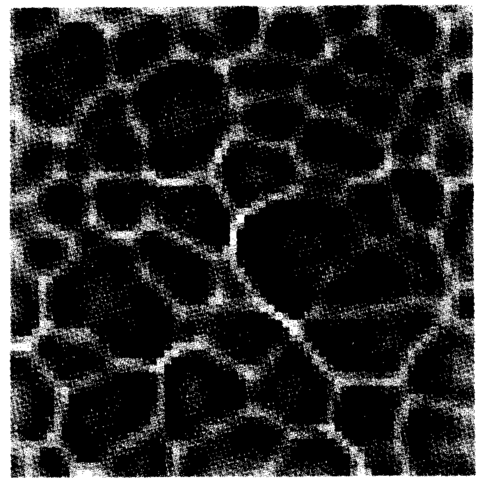

Fig. 2. Grey level picture of R in a (160×160) domain around the deepest minimum recorded during the (5120×5120)-experiment ($c_1 = 2.0$, $c_3 = 0.75$, $t = 6118$; $R = 0.712 \to$ black, $R = 1.125 \to$ white). The life-time of such "anomalies" is usually short ($\Delta t \sim 10$). The "ordinary" cells contribute to the central part of the histogram of R.

which achieves an optimum between the destabilizing second-order term and the stabilizing fourth-order term in the linear part of (4). The cells actually observed precisely have a typical size of the order of $\lambda_{\max}$. They are best observed in snapshots of the phase gradient $\nabla\phi$, or, equivalently, of the magnitude R, since, at lowest order in $\nabla\phi$, the magnitude fluctuations defined through $R = R_0 + \delta R$, are "slaved" to the phase gradient according to:

$$\delta R = -\tfrac{1}{2}(\nabla\psi)^2 - \tfrac{1}{2}c_1\nabla^2\psi\,. \qquad (8)$$

Since $\lambda_{\max}$ diverges as $|D|^{-1/2}$ when approaching the BF line, the simulation of truly large systems (i.e., of size much larger than $\lambda_{\max}$), remains out of reach in this region of parameter space. Sufficiently far from the BF line, though, current computer power permits the study of systems large enough to accomodate thousands of cells. In this limit of many cells, as is considered here, phase turbulence is an extensively chaotic regime (as demonstrated for $d = 1$ by Egolf and Greenside), and statistically stationary dynamics is observed.

In this paper, we restrict ourselves to the line $c_1 = 2$ in the (c_1, c_3) plane, i.e., we only consider c_3 increasing from the BF value $c_3 = 0.5$ up. As already reported in our numerical exploration [12], defects nucleate rapidly for $c_3 > 0.78$. Below this value, phase turbulence is only metastable in the sense that it persists over long periods of time but does not withstand the introduction of a strong local perturbation (e.g., a defect), after which amplitude turbulence develops irreversibly.

The simplest way to study the persistence of phase turbulence is to monitor $R_{\min}$, the minimum of R over the surface of the system as a function of time. The direct study of the phase gradient, though in some respect more directly related to our problem, is computationally more expensive and has not been systematically performed, taking advantage of Eq. (8), which relates $\nabla\phi$ to R (see, however, Fig. 7 below). Time series of $R_{\min}$ have been recorded for system sizes varying from 80×80 to 5120×5120. [1] Fig. 3 displays the time-series of $R_{\min}$ for $L = 1920$ and $c_3 = 0.70$, sampled every $\Delta t = 1$. After a short size-independent transient ($t < 700$ when starting from a nearly uniform initial conditions), the field R reaches a statistically stationary regime, with well-defined averages and fluctuation levels. Strictly speaking, since the sampling is discrete in time and involves evaluations of R only at the collocation points, the absolute minimum is missed, but "typical minima" are captured. [2]

Fig. 4 displays $\langle R_{\min}\rangle_T$, the average of $R_{\min}$ over a time T, as a function of $\ln(L)$ for $T \simeq 50\,000$ and for $c_3 = 0.70$ and 0.75. $\langle R_{\min}\rangle_T$ decreases logarithmically with L close to the breakdown boundary ($c_3 = 0.75$), and more slowly further away ($c_3 = 0.70$). A complementary way to analyze the time series of $R_{\min}$ consists of looking at the variation of $\langle R_{\min}\rangle_T$ with T at given size L. The time-series of the experiments at $c_3 = 0.75$ of Fig. 4 were divided into successive sections of duration T, yielding, for each size L, a set of realizations of $\langle R_{\min}\rangle_T$, which was then averaged. Fig. 5 shows the logarithmic variation with L of this quantity $\langle\langle R_{\min}\rangle_T\rangle$.

These results can be fitted by:

$$\langle R_{\min}\rangle_T\,(L) \sim -K_L \ln(L) \quad \text{and}$$
$$\langle\langle R_{\min}\rangle_T\rangle(T) \sim -K_T \ln(T)$$

with

$$K_L = 0.0164 \pm 0.0009 \quad \text{and}$$
$$K_T = 0.0077 \pm 0.0002\,,$$

i.e., roughly $K_L = 2K_T$.

To get a deeper insight into this behavior, we studied the statistics of R in greater detail. Fig. 6 displays the histogram of R (lin–log scales) for $c_3 = 0.70$ and $L = 1920$. The shape of the central part for $R \sim 1$ does not change as parameters are modified. It simply reflects the general tessellated organization of the R field described in the beginning of this section (see Fig. 2). The tail of the histogram at low values of R is of primary interest here since the breakdown process involves small values of the magnitude (large values of the phase gradient). As already noticed for the one-dimensional case [8], the behavior of this tail changes with the relative distance to the BF line: for $c_3 = 0.70$ this tail is well approximated by a parabola, suggesting a Gaussian behavior (Fig. 6, right, and Fig. 7). Closer to the breakdown value, for $c_3 = 0.75$, the histogram develops an exponential tail, as shown in Fig. 8. The left part of this figure clearly shows that the shape of the tail is independent of the system size, and is explored further and further down as L increases (at fixed T).

The behavior of the tail of the histogram can be related to the scaling of $\langle R_{\min}\rangle_T$ with L and T. The low values of R are due to "anomalous" cells of the kind shown in the middle of Fig. 2. From numerical evidence, we can assume that such cells are scattered

[1] The simulations have been performed using a standard Fourier-based pseudo-spectral method adapted to periodic boundary conditions, with exact integration of the linear terms in (1) and slaving of fast decaying modes, as proposed in: U. Frisch, Z.-S. She and O. Thual, Viscoelastic behaviour of cellular solutions to the Kuramoto–Sivashinsky model, J. Fluid Mech. 168 (1986) 221. Initial conditions and space–time resolution were chosen appropriate to the concerned regime. For the phase regime, which is only slowly varying, relatively large space steps δx, up to 2.5, could be used but they had to be reduced down to $\delta x \sim 1$ when defects were present. Usually, the time step $\delta t = 0.05$ was taken, guaranteeing a sufficiently faithful dynamics in all cases.

[2] A similar analysis was also performed by measuring the minimum of R in portions of size $L \times L$ extracted from bigger systems. Values of $\langle R_{\min}\rangle_T\,(L)$ obtained this way are undistinguishable from those measured in systems of total size $L \times L$.

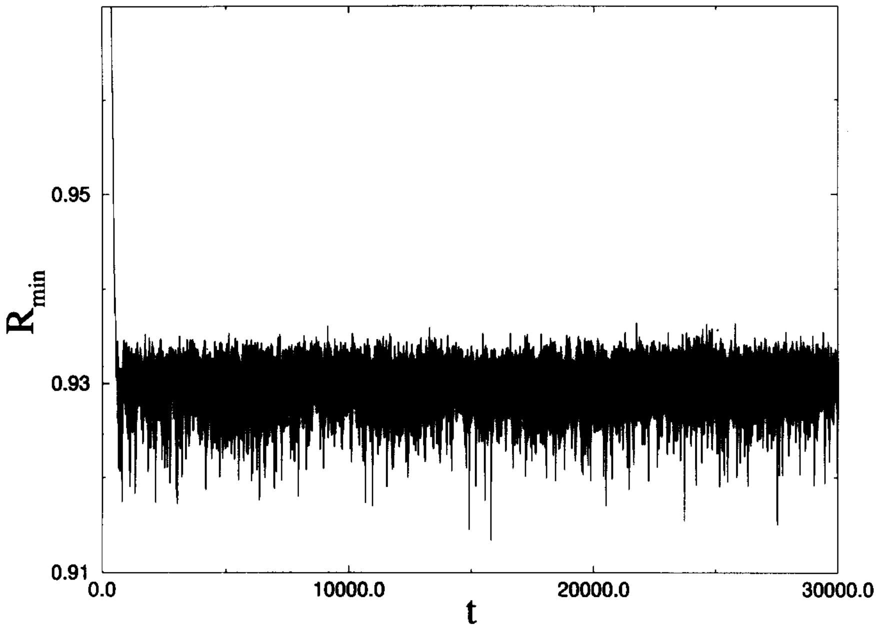

Fig. 3. Minimum of R over the system (size 1920×1920), recorded as a function of time every $\Delta t = 1$ for $c_1 = 2$ and $c_3 = 0.7$.

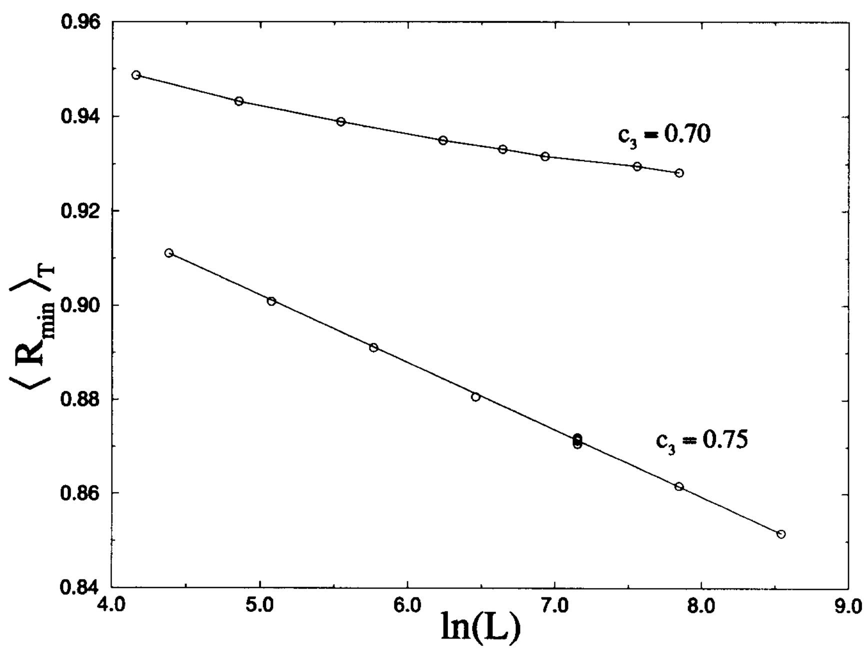

Fig. 4. Log–lin plot of the time average of $R_{\rm min}$ as a function of L for $c_3 = 0.70$ and $c_3 = 0.75$ ($c_1 = 2.0$). For $c_3 = 0.70$ the decrease is slower than logarithmic. Statistics begins at $t = 5000$ and is cumulated during a time $T \simeq 50\,000$. The dispersion of the results for $L = 1280$ and $c_3 = 0.75$, which correspond to five independent runs, gives an idea of the error bars.

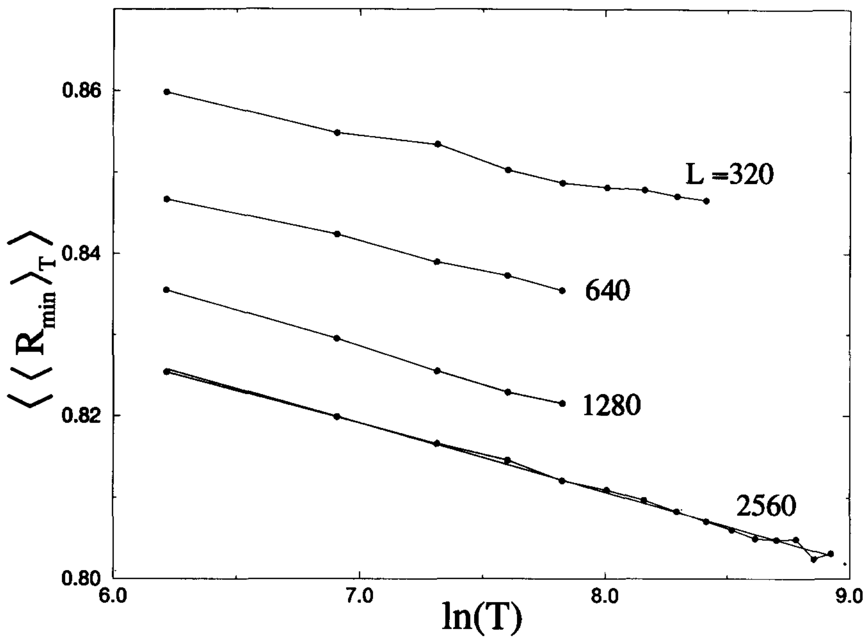

Fig. 5. Log–lin plot of the average of $R_{\min}$ over periods of time T as a function of T for $c_1 = 2.0$, $c_3 = 0.75$ and $L = 320\,640$, 1280 (average over 5 independent runs), and 2560 (2 runs).

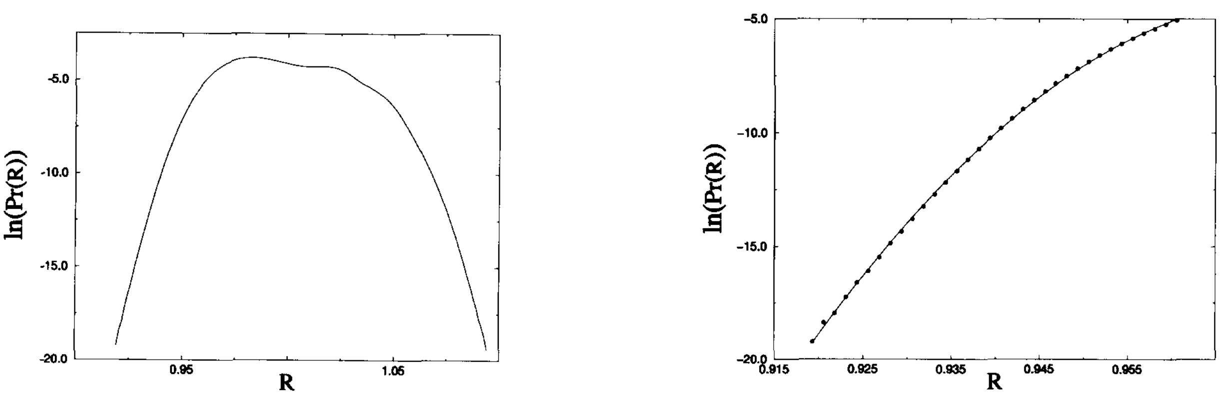

Fig. 6. Lin–log plot of the histogram of R for $c_1 = 2$ and $c_3 = 0.7$ in a system of size 1920×1920. Averaging was performed over samples taken every $\Delta t = 1$ from $t = 11\,000$ to $t = 31\,000$). Left: Complete histogram. Right: Tail of the histogram fitted against a parabola corresponding to a Gaussian behavior.

randomly over the surface of the system with some low density and that they have a finite lifetime, so that configurations sufficiently far apart in time (and space) are independent. From a statistical point of view, this is equivalent to considering the dynamics of extreme events as drawing at random a number $n_L \propto L^2$ of anomalous cells, and repeating this process at some fixed frequency (i.e., a number $n_T \propto T$ of such draws is performed over a given time interval T).

Assuming the exponential tail of the histogram of R, fitted to:

$$\Pr(R) \propto \exp(-K_R(R^* - R)),$$

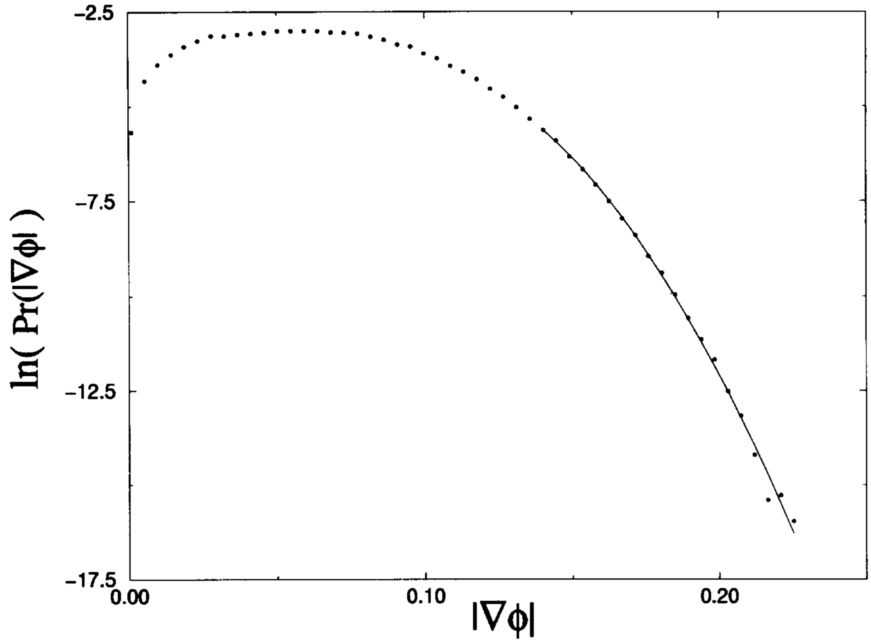

Fig. 7. Lin–log plot of the histogram of $|\nabla\phi|$ for the same run as in Fig. 6, with averaging over samples taken every $\Delta t = 500$ from $t = 2500$ to $t = 31\,000$. The line is a tentative fit of the tail against a parabola corresponding to a Gaussian behavior mirroring that of R.

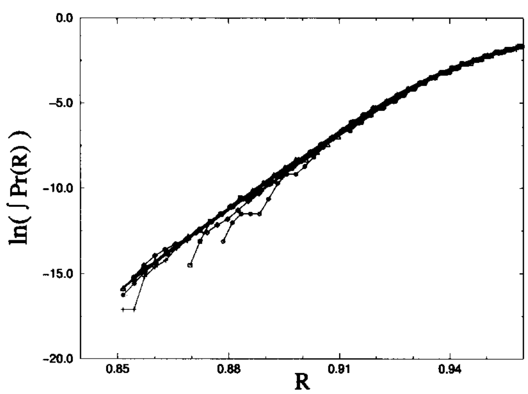

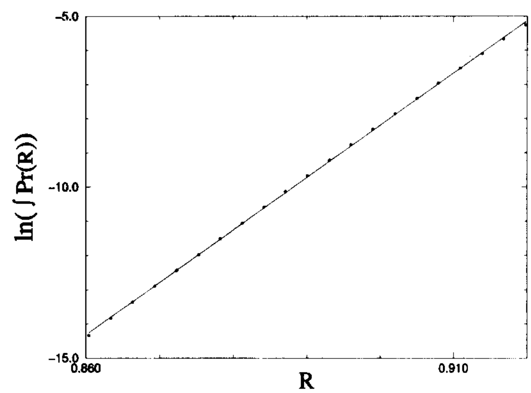

Fig. 8. Left: Lin–log plot of the tail of the cumulated histograms of R for $c_1 = 2.0$, $c_3 = 0.75$ and $L = 80$ (circles), 160 (squares), 320 (diamond), 640 (plus sign), 1280 (triangle up), 2560 (asterisk), and 5120 (thick line). Right: Lowest part of the tail for $L = 5120$, fitted to a straight line corresponding to an exponential behavior. The histograms were recorded at a rather low frequency to save computer resources. To palliate the lack of data, we have chosen to display the – less noisy – integrated histogram of R, which does not affect the exponential behavior observed.

the probability for R to remain larger than $R_{\min}$ after $n_L n_T \propto L^2 T$ draws is then proportional to:

$$\left[\int_{R_{\min}}^{R^*} \exp(-K_R(R^* - R))\,\mathrm{d}R\right]^{L^2 T}$$

$$\propto \left[1 - \exp(-K_R(R^* - R_{\min}))\right]^{L^2 T}$$

$$\propto \left[1 - L^2 T \exp(-K_R(R^* - R_{\min}))\right].$$

This probability vanishes, i.e., R is almost surely smaller than $R_{\min}$ for

$$\exp(-K_R(R^* - R_{\min})) \propto (L^2T)^{-1}$$

or

$$R_{\min} \sim \text{Cst.} - (1/K_R)\ln(L^2T),$$

a result consistent with the analysis of $\langle R_{\min}\rangle_T$. Moreover, fitting the tail of the histogram of Fig. 8 (right), one gets $K_R = 153 \pm 2$, which yields $\frac{1}{2}K_L = K_T = 1/K_R \simeq 0.0065$, in good quantitative agreement with the above-mentioned values. This is an a posteriori confirmation of the picture emerging from the idea that the extreme events of interest are *local* in space and time and that they occur *randomly* in space–time. We note finally that the slower-than-logarithmic decrease of $\langle R_{\min}\rangle_T$ as a function of L or T closer to the BF line (Fig. 4, $c_3 = 0.70$) is also consistent with the quasi-Gaussian behavior of the histogram (Fig. 6).

The statistical analysis presented above has revealed regular scaling properties for the quantities of interest, and it is tempting to extrapolate these numerical results to the infinite-size, infinite-time, thermodynamic limit.

When and how does the breakdown of phase turbulence occur? Numerical experiments such as those reported in [8] and [12] suggest that, at given parameter values, there exists a nonvanishing "critical" magnitude R_c (and, correspondingly, a finite critical phase gradient) beyond which the system is *locally* attracted to a defect solution. We can thus define the probability of breakdown p_b as the probability for R to reach values smaller than R_c (here we estimate $R_c \sim 0.6$ for the range of c_3 values considered).

The numerical evidence presented above revealed that, at fixed parameter values, there exists a unique histogram of R whose —exponential— tail is revealed when increasing L or T. This is true for $c_3 = 0.75$. For smaller values of c_3, we believe this is also the case, although, due to the divergence of scales in this limit, we are obviously unable to provide numerical evidence justifying this. At any rate, exponential tails are easily observed in the breakdown region. We then deduce that for parameter values, system sizes L, and integration times T for which the histogram of R shows an exponential tail, we can define a line of "sure breakdown" ($p_b = 1$) in the (c_1, c_3) plane once the dependence of K_R, R^*, and R_c with parameters is determined. In fact, following the hypothesis that exponential tails eventually develop for any c_3 value provided that L or T is large enough, we expect that the dependence of R_c and R^* on c_3 is weak and that only K_R varies substantially, probably diverging when the BF line is approached. Let us remark finally that the experimental protocol used for the determination of lines L_1, L_3, and L in [7] and [12] (see caption of Fig. 1), is equivalent to the above definition of the line of sure breakdown.

In the above argument, we followed the "natural" trend indicated by our numerical results and discussed their consequences and meaning when extrapolating them to the thermodynamic limit. That notwithstanding, we naturally cannot exclude, on the sole basis of numerical experiments of this kind, the possibility that the observed scaling properties do *not* carry to infinity (in space and/or time). Indeed, in such a deterministic setting – fundamentally different from stochastic systems submitted to unbounded noise – , there may well be cut-off mechanisms which "prevent" the occurrence of (too) extreme events. If such were the case – but, again, we did not see any evidence for it – , then phase turbulence might exist in the infinite-size, infinite-time, thermodynamic limit, at least in some region of parameter space.

4. Effective large-scale description of phase turbulence

As long as the breakdown of phase turbulence remains of negligible probability, one can try to reduce the dynamics of the complex amplitude A to that of the large-scale fluctuations of its phase ϕ together with an "effective noise". In such a Langevin-like approach, the local fluctuations, and in particular those of R, would be accounted for by the "microscopic" noise term since they take place on scales of the order of the cell size (see Figs. 2 and 3 in [12]).

Furthermore, when considering the fluctuations of the phase field, the problem of the effective large-scale description is similar to the one posed in the context of the KS equation or any other *fluctuating interface* problem. Unwinding the phase variable on the real axis as a coordinate in a direction transverse to the physical space (a third dimension here), the phase advance is turned into the progression of an d-dimensional surface in a $(d+1)$-dimensional space. This approach leads to investigate the (possible) scaling behavior of the phase interface. For an interface of position $h(\mathbf{x}, t)$, these properties are expressed by the dilatation invariance according to

$$h(l\mathbf{x}, l^z t) = l^\zeta h(\mathbf{x}, t), \tag{9}$$

where l is a similarity factor, and ζ and z are known as the "roughness" and "dynamical" exponents [23]. A large body of work on fluctuating interface problems has brought evidence that there exist large universality classes characterized by the values of the (dimension-dependent) scaling exponents ζ and z. To determine which universality class a given problem belongs to, one should study the series of moments of $h(\mathbf{x}, t)$. In practice it is often the case that even the double correlator $\langle h(\mathbf{x}, t)h(\mathbf{x}', t')\rangle$ is difficult to estimate, and one usually considers more global quantities such as the width $w(t)$ of the interface defined from the mean square of the height distribution [23].

$$w(t)^2 = \left\langle (h(\mathbf{x}, t) - \langle h\rangle_\mathbf{x})^2 \right\rangle_\mathbf{x},$$

where $\langle\ldots\rangle_\mathbf{x}$ denotes space average. Scale-invariance of $h(\mathbf{x}, t)$ (Eq. (9)) implies that

$$w(t) \sim L^\zeta \mathcal{G}(t/L^z),$$

where $\mathcal{G}(u)$ is a function whose asymptotic behavior must be given by

$$\mathcal{G}(u \ll 1) \sim u^{\zeta/z},$$
$$\mathcal{G}(u \to \infty) = \mathrm{Cst}.$$

The large-scale properties of many microscopic fluctuating interface models can be described by an effective stochastic partial differential equation most often called the Kardar–Parisi–Zhang (KPZ) equation [24]. The KPZ model reads:

$$\partial_t h = \nu\nabla^2 h - \tfrac{1}{2}\lambda(\nabla h)^2 + \xi(\mathbf{x}, t), \tag{10}$$

where $\xi(\mathbf{x}, t)$ is a δ-correlated Gaussian noise with

$$\left\langle \xi(\mathbf{x}, t)\xi(\mathbf{x}', t')\right\rangle_\xi = 2D\delta(\mathbf{x} - \mathbf{x}')\delta(t - t') \tag{11}$$

(here $\langle\ldots\rangle_\xi$ denotes the average over realizations and D measures the intensity of the noise). The scaling exponents for the KPZ class are known exactly for $d = 1$: $\zeta = \frac{1}{2}$ and $z = \frac{3}{2}$ [24]. For higher dimensions, only numerical results are available. For $d = 2$, one expects $\zeta \simeq 0.39$ and $z \simeq 1.61$ [25]. As a matter of fact, much more is known about the dynamics of interfaces governed by the KPZ equation at large scales. In particular, during an experiment initiated with a flat interface, gradients build up progressively and the corresponding nonlinearities are not effective from the start. A preliminary phase takes place, usually called the "linear," "free-field," or "Edwards–Wilkinson" regime [26], during which one may observe a scaling behavior consistent with the simple, exactly-solvable case where nonlinearities are negligible, i.e., $\lambda = 0$ in (10). One then gets $z = 2$ (i.e., a standard diffusive behavior) and $\zeta = (2 - d)/2$. The two-dimensional case is marginal ($\zeta = 0$) and logarithmic corrections are expected. It is only when the system size is larger than a well-defined crossover scale L_c and when it can be observed for times longer than a crossover time t_c, that the nontrivial scaling properties of KPZ are observed.

The KPZ class is characterized by three important ingredients. First, there must be, at large-scales, an effective diffusion. In the context considered here, this may appear as a major problem since phase turbulence is essentially linked to a negative phase diffusion coefficient D. However, Chow and Hwa have given, for the KS equation, a convincing account of how a positive diffusion constant may arise at large scales. The second characteristic ingredient of KPZ is the quadratic nonlinear term $(\nabla\phi)^2$. In phase turbulence, this nonlinear term is, in some sense, naturally expected: it is "built-in microscopically" as seen from the phase dynamics approach (see Section 2). The third ingredient is the nature of the effective noise ξ. It is by no means obvious, in a deterministic setting such as considered here, that the effective noise at large scales is Gaussian and δ-correlated. This is all the more crucial than it was shown that correlated noise influences the scaling exponents [27].

Previous work on phase turbulence has nevertheless brought some evidence for the relevance of the KPZ class, although this is still a matter of controversy.

The KS Eq. (6) has been the subject of numerous theoretical and experimental studies in this context. In one space dimension, all the results obtained lean toward the relevance of KPZ as the effective large-scale description [28–33]. Yet, no direct, full-fledged, numerical evidence of the nonlinear scaling regime has been given so far, with the exception of [30] where the crossover was reached. For $d = 2$, the matter is even less settled, with an ongoing controversy over the right asymptotic scaling behavior [35–38] that numerical results are so far unable to resolve definitively.

Recently, phase turbulence in the one-dimensional CGL equation has also been numerically tested against KPZ scaling, together with general conjectures about the behavior of space and time correlations for the field A in that hypothesis [39]. The recorded behavior was consistent with the linear regime, but the nonlinear scaling regime was not observed. Further results by one of us [34] on larger systems using a higher accuracy code did reveal the expected scaling exponent $\zeta/z = \frac{1}{3}$ beyond crossover scales actually smaller than those estimated in [39]. Here, we consider the two-dimensional case.

The continuous phase interface was extracted at regular intervals in time during the same runs as those presented in Section 3. Large-scale fluctuations, although of rather limited amplitude, are easily observed (see Fig. 3(b) in [12]). The full distribution of the phase variable (not recorded systematically) was always found to be reasonably well fitted against a Gaussian (Fig. 9). In the following, only data for the width w of the phase distribution is presented. [3]

Moreover, we mostly studied the parameter values $c_1 = 2$ and $c_3 = 0.75$ in order to have the largest possible effective aspect-ratio ($L/\lambda_{\max}$) without reaching the breakdown limit. For all sizes studied but the largest one (5120×5120), runs could be followed long enough to observe the saturation of the growth of w. Fig. 10 shows the case of the largest system considered, for which, naturally, the growth behavior is the least noisy and can be observed during the longest time. A clear logarithmic law is observed. The same behavior was observed for all sizes $L \geq 640$. When fitted (poorly) against power laws, ridiculously small exponents are obtained. The same conclusion applies to the scaling of the saturated width with L (Fig. 11). These logarithmic dependences are a clear signature of the linear regime [40]. As is the Gaussian character of the full phase distribution (Fig. 9), since one expects non-vanishing values of the skewness in the nonlinear regime [23].

Following [40,25], we now estimate the effective parameters ν, λ, and D, of (10).

In the linear regime, in the limit of large sizes, one expects the width w to grow as [40].

$$w^2 = \frac{D}{4\pi\nu}\left[\ln(\kappa t) + \mathrm{O}\left(\frac{\nu t}{L^2}\right)\right], \tag{12}$$

where κ is a constant homogeneous to t^{-1} that reads

$$\kappa = 2\pi^2 \exp(\gamma)\frac{\nu}{a^2}.$$

Here a is a "microscopic" length and $\gamma = 0.5772\ldots$ is Euler's constant. Fitting the results in Fig. 10 against $A\ln(t) + B$ one obtains:

$$A = 0.019641 \pm 0.00003, \qquad B = 0.0740 \pm 0.003,$$

which leads to the estimates:

$$\frac{D}{\nu} \simeq 0.25, \qquad \frac{\nu}{a^2} \simeq 1.23,$$

provided that the second term in (12) is indeed smaller than the first one (see below).

In the same way, the dependence of the saturated width with L in the linear regime is given by

$$w^2 = \frac{D}{2\pi\nu}\ln(L/a) + \mathrm{O}(1). \tag{13}$$

A fit of the results of Fig. 11 against $A\ln(L) + B$ yields:

$$A = 0.0378 \pm 0.0030, \qquad B = -0.021 \pm 0.017,$$

giving

$$\frac{D}{\nu} \simeq 0.24.$$

[3] Results for the power spectra of the phase field $\phi = \arg A$ or the full field A, and for the corresponding correlation functions, were found to be more difficult to interpret, which is understandable since they carry a much richer information than the simple quantity w [39].

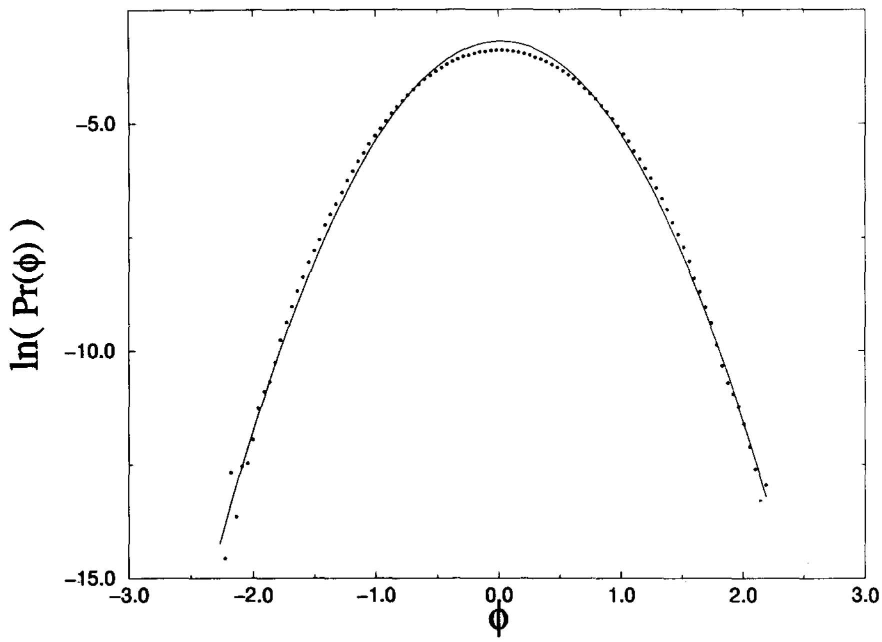

Fig. 9. Lin–log plot of the instantaneous distribution of the phase $\phi = \arg A$ over the (5120×5120) system for $c_1 = 2.0$ and $c_3 = 0.75$, at time $t = 25\,000$. The fit against a parabola indicating Gaussian behavior is satisfactory. The skewness is negligible.

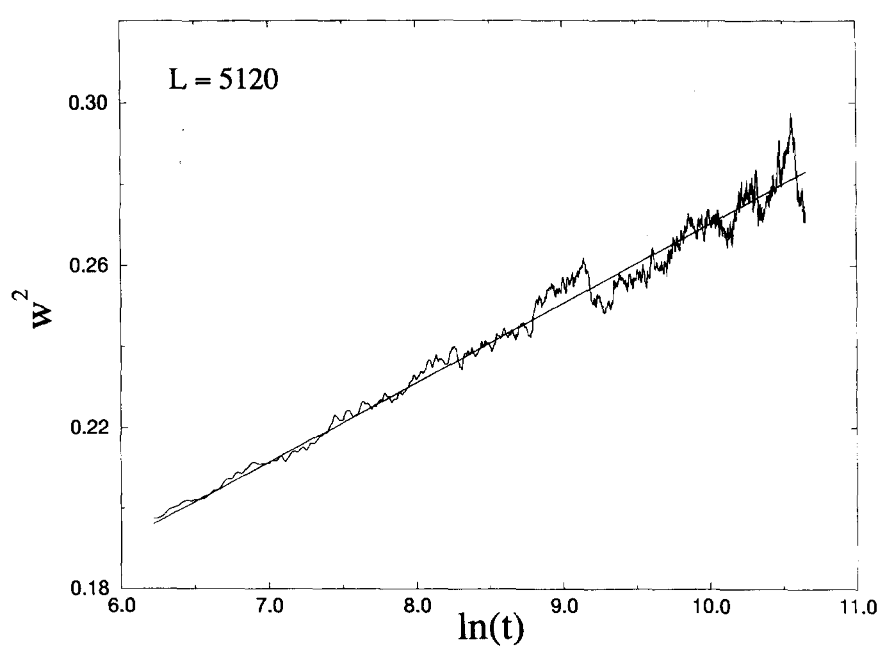

Fig. 10. Mean-square width w^2 of the phase distribution as a function of $\ln(t)$ during the growth stage for $c_1 = 2$, $c_3 = 0.75$ and $L = 5120$, following a slightly-perturbed homogeneous initial condition.

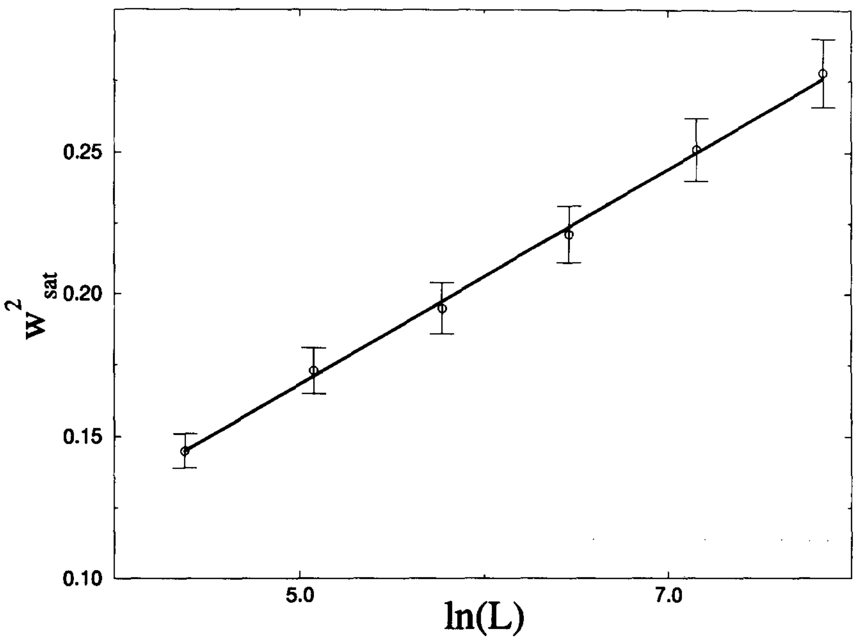

Fig. 11. Time-averaged mean-square width $w^2_{\rm sat}$ of the phase distribution after saturation as a function of $\ln(L)$ for L varying between 80 and 2560. The error bars have been determined from the average over five independent simulations with $L = 1280$.

We first note that the two estimates of D/ν are fully consistent with each other. The above fit should in principle also provide an estimate of a. This is misleading since in (13) the "effective initial" value w_0 of the width is not taken explicitly into account. In fact, w_0 can be seen as the typical width for a system of size a, i.e., w_0^2 is given by the O(1) term in (13). We thus need an independent estimate of a or w_0 to be able to complete our estimates of the effective KPZ parameters.

The most "natural" microscopic scale for phase turbulence should not be much different from the cell size $\lambda_{\max}$. Taking simply $a \simeq \lambda_{\max} \simeq 22$.[4] and injecting this value in (13), together with the estimate of $D/\nu \simeq 0.25$, we get

$$w^2 - w_0^2 \simeq 0.0378(\ln(L) - 3.1)\,.$$

Using values of w^2 extracted from our results finally yield: $w_0^2 \simeq 0.089$, which is small compared to the typical values of w^2 measured, validating Eq. (13).

In fact, it is possible to derive an a priori estimate for w_0 from the phase dynamics analysis of CGL, through its KS approximation. The typical scale of the phase field (squared) is given by: $w_0^2 \simeq (D/g_0)^2 \simeq 0.033$ at the parameter values considered here. This value is of the same order of magnitude as the value determined from the analysis above, following our choice of a.

Accepting these values, one obtains

$$\nu \simeq 600 \quad \text{and} \quad D \simeq 150\,.$$

Finally, coming back to Eq. (12), we note that using $a \simeq \lambda_{\max}$ yields typical values of the $(\nu t/L^2)$ smaller than the dominant term, in consistency with our analysis.

The observation of the linear regime does not imply that the nonlinear term in (10) is absent, but simply that it is irrelevant at the scales considered here. The value of the coefficient λ of this nonlinear term is usually estimated by considering "tilted" interfaces. It was shown in [23] that

$$\lambda = \left.\frac{\partial^2 v}{\partial q^2}\right|_{q=0},$$

[4] An experimental determination of the average cell-size, from the spatial power spectra, yields: $\lambda_{\max} \simeq 19$, in good agreement with the "theoretical" value.

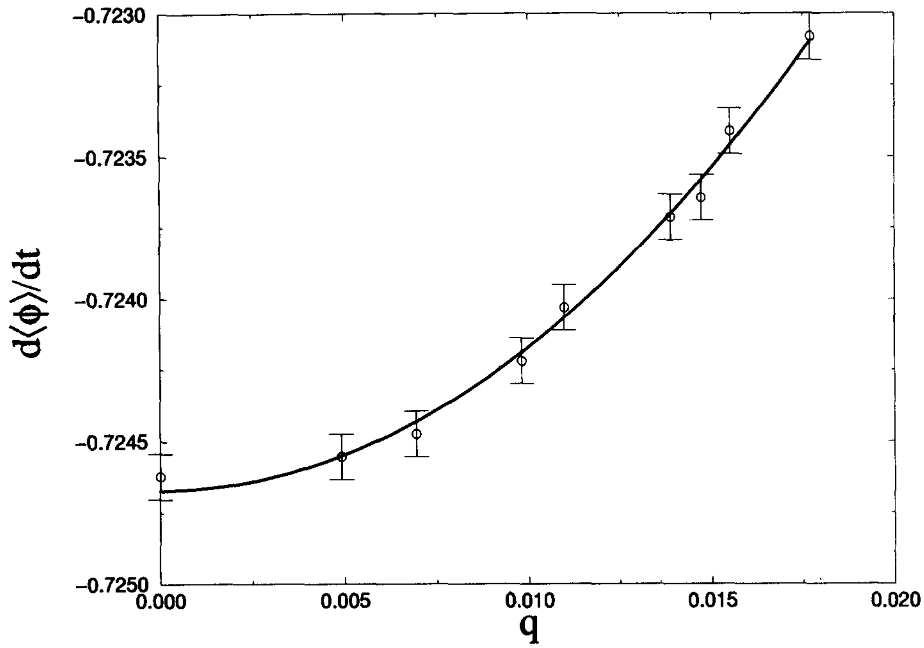

Fig. 12. Variation of the winding rate as a function of $q = |\mathbf{q}|$ and fitted quadratic dependence $A+Bq^2$. Statistical errors were estimated by performing five experiments with mode $(1,2)$ yielding a rate -0.72412 and an unbiased standard deviation $\sigma_{n-1} = 7 \times 10^{-5}$. This value was then used uniformly for all the other entries, which is probably too conservative since the fitted curve goes easily through all the error bars.

where q here is the average slope of the interface and $v(q)$ the corresponding velocity.

In the present context, one has to study phase turbulence with nonzero winding number: solutions evolving from initial conditions close to a plane wave with nonzero wavevector $\mathbf{q}$ compatible with the periodic boundary conditions ($\mathbf{q} = (n_x, n_y) \times 2\pi/L$) and corresponding to tilted interfaces with an average slope $q = |\mathbf{q}|$. Their velocity is nothing but the winding rate: $v = \mathrm{d}\langle\phi\rangle_{\mathbf{x}}/\mathrm{d}t$. Results obtained for small wavenumbers are shown in Fig. 12. They are well approximated by a parabola $A + Bq^2$ with:

$$A = -0.7247 \pm 0.0001\,, \qquad B = 5.03 \pm 0.25\,.$$

The estimate for λ then derives immediately from this fit,

$$\lambda \simeq 10\,.$$

This value is significantly larger than the "bare" value $2g_0 = 2(c_1 + c_3) = 5.5$ given by the phase velocity ω_q of the planewave solutions (2,3). A similar discrepancy was reported for the KS equation [30,37] and for the one-dimensional CGL equation [39]. A detailed study of this problem for the one-dimensional case [34] has shown that this is *not* a numerical effect. Increasing the resolution, the measured value of λ converges to a limit distinct from the bare value. The intrinsic spatio-temporal chaos of phase turbulence has therefore a nontrivial effect on the average velocity of the phase interface. In a given numerical context, the experimentally-determined value of λ – which incorporates the intrinsic noise and the effect of numerical truncation – reflects the actual noise in the discretized system evolving on the computer. To be consistent, one should thus keep this value together with those of the other parameters of KPZ evaluated in the same conditions.

Finally, the so-called coupling constant is evaluated.

$$g = D\lambda^2/\nu^3 \sim 10^{-4}\,.$$

The value of the crossover length $L_c = a\exp(8\pi/g)$ beyond which the nontrivial scaling regime is expected [40] is astronomically large, and certainly much larger than the largest size considered here.

Even though this estimate is subjected to large error bars given the exponential dependence of L_c on g, the fact remains that the crossover regime is out of reach of the power of current computers. This result is of course consistent with our observation of the sole linear regime even for the largest size considered. Our estimates of ν and D are much larger than those found in the one-dimensional case [30,33,39]. We attribute this discrepancy to the much greater "rigidity" of the phase interface in two dimensions.

5. Summary and conclusion

We have presented extensive numerical simulations of the two-dimensional CGL equation in a parameter range where phase turbulence is observed. Two central questions were addressed:
- Does phase turbulence exist in the infinite-size, infinite-time, thermodynamic limit?
- Is the KPZ equation the relevant Langevin-like large-scale description of phase turbulence?

It should not come as a surprise that definitive answers to these questions have not emerged out of the numerical approach taken here. But our careful statistical analysis did provide a clearer view of these problems, together with some plausible answers.

Extrapolating the size- and time-effects revealed by the statistical analysis of $R(\mathbf{x}, t)$, we conclude that the probability of breakdown of phase turbulence, i.e., of the nucleation of a defect, may be minute but is always finite. But we cannot exclude a scenario in which, in a region of parameter space, "regularizing" mechanisms deterministically prevent the occurrence of the extreme fluctuations which would have led to breakdown. If such were the case, phase turbulence would exist in the thermodynamic limit. Our results also suggest the dependence of this probability on system size, integration time and, to some extent, parameters. In this respect, it would be interesting to try to check the conjecture made above according to which the histogram of R would develop an exponential tail as close as desired from the BF line for large enough system sizes and/or integration times.

To complete our analysis of the statistics of R, the (localized) events characterizing the breakdown should be studied in detail. The "anomalous" cells could be approached as special solutions in the framework of low-dimensional dynamical systems. Such a study would put the estimation of the critical magnitude R_c on firm ground. More easily, one could investigate the statistical properties of these extreme events – from which the coefficients K_L and K_T introduced in Section 3 derive –, and a precise link with the statistical behavior of R – in particular the coefficient K_R – could then be drawn.

The large-scale properties of phase turbulence in the CGL equation, a spatio-temporal chaos regime produced by a deterministic system, are reasonably well described within the framework of a Langevin formalism: local chaotic fluctuations are well accounted for by an effective noise. Experiments on tilted interfaces have produced evidence for the existence of the $(\nabla\phi)^2$ nonlinear term in the effective Langevin equation, one of the characteristic features of the KPZ model. Our study of the scaling properties of the "phase interface" have revealed a behavior characteristic of the Edwards–Wilkinson equation, establishing the existence of an effective positive diffusion constant ν, and the uncorrelated nature of the effective noise. These properties are in fact fully consistent with KPZ, since the observed scaling is, of course, that of its so-called linear regime, and since, furthermore, the crossover scale L_c, beyond which the nonlinear scaling regime could be observed in theory, has been estimated to be much larger than the largest size considered here.

In view of the results presented here, if the validity of the KPZ description seems likely, it is not ensured. Even when assuming the relevance of KPZ, the expected nonlinear regime might not be observable at all: the crossover scales could be beyond the limit of "sure breakdown." This is one of the reasons why it may be important to study the variation of the effective KPZ parameters with the parameters of CGL (here with c_3), and, in particular, how the (estimated) crossover scale and the breakdown probability vary when approaching the BF line.

This could also, in turn, bring new insights into the corresponding problem for the KS equation in two dimensions, which appears as a limit case in this context. Is phase turbulence in CGL different from phase turbulence in KS? It was shown in [8] that, for $d = 1$, the local dynamics is very different for the two models. For $d = 2$ and for the large-scale properties, this is much less clear. Without entering the controversy surrounding the two-dimensional KS equation, we note as a fact that the results of Fig. 4 do *not* fit well against the scaling $w \sim \ln(\ln(L/L^*))$, which was proposed in [35] for the latter equation.

At any rate, the difficulties encountered are certainly due to the marginal character of the two-dimensional case. A more precise approach than the global one taken here, for example along the lines of [32], could be followed to decide whether the logarithmic scalings observed can really be attributed to the irrelevance of the nonlinear term in KPZ or results from some other property, such as the nonlocality of couplings in k-space.

We hope that this work will help strengthen the current trend toward the extension of methods and concepts of equilibrium statistical mechanics and field theory to large out-of-equilibrium dynamical systems, for which space–time chaos in "extended" systems is one of the most promising areas.

Acknowledgements

We thank Joachim Krug and Lei-Han Tang for fruitful discussions. The extensive numerical simulations reported here have been made possible thanks to a greatly-appreciated, massive CRAY CPU time allocation attributed by the "Conseil Scientifique pour le Calcul Centralisé" of the "Direction des Sciences de la Matière – Commissariat à l'Énergie Atomique."

References

[1] A.C. Newell, The dynamics of patterns: A survey, in [2].
[2] J.E. Wesfreid, H.R. Brand, P. Manneville, G. Albinet and N. Boccara, eds., Propagation in Systems Far from Equilibrium (Springer, Berlin, 1988).
[3] W. van Saarloos, The complex Ginzburg–Landau equation for beginners, in [4].
[4] P.E. Cladis and P. Palffy-Muhoray, eds., Spatiotemporal Patterns in Nonequilibrium Systems (Addison–Wesley, Reading MA, 1994).
[5] Y. Kuramoto, Chemical Oscillations, Waves and Turbulence (Springer, Berlin, 1984).
[6] M.C. Cross and P.C. Hohenberg, Pattern formation outside of equilibrium, Rev. Modern Phys. 65 (1993) 851.
[7] B.I. Shraiman, A. Pumir, W. van Saarloos, P.C. Hohenberg, H. Chaté and M. Holen, Spatiotemporal chaos in the one-dimensional complex Ginzburg–Landau equation, Physica D 57 (1992) 241.
[8] H. Chaté, Disordered regimes of the one-dimensional complex Ginzburg–Landau equation, in [4].
[9] H. Chaté, Spatiotemporal intermittency regimes of the one-dimensional complex Ginzburg–Landau equation, Nonlinearity 7 (1994) 185.
[10] G. Huber, P. Alstrøm and T. Bohr, Nucleation and transients at the onset of vortex turbulence, Phys. Rev. Lett. 69 (1992) 2380.
[11] G. Huber, Vortex solids and vortex liquids in a complex Ginzburg–Landau equation, in [4].
[12] H. Chaté and P. Manneville, Phase diagram of the two-dimensional complex Ginzburg–Landau equation, Physica A 224 (1996) 348.
[13] P. Coullet, L. Gil and J. Lega, Defect mediated turbulence, Phys. Rev. Lett. 62 (1989) 1619.
[14] Y. Kuramoto, Diffusion-induced chaos in reaction systems, Progr. Theoret. Phys. (Supp.) 64 (1978) 348.
[15] D.A. Egolf and H.S. Greenside, Characterisation of the transition from defect to phase turbulence, Phys. Rev. Lett. 74 (1995) 1751.
[16] H. Brand, Phase dynamics – a review and a perspective, in [2].
[17] J. Lega, Défauts topologiques associés à la brisure de l'invariance de translation dans le temps, Thèse de Doctorat, Université de Nice (1989).
[18] A.C. Newell, Envelope equations, Lectures in Applied Mathematics, Vol. 15 (American Mathematical Society, Providence, RI, 1974) pp. 157.
[19] Y. Kuramoto and T. Tsuzuki, Reductive perturbation approach to chemical instabilities, Progr. Theoret. Phys. 52 (1974) 1399; G.I. Sivashinsky, Nonlinear analysis of hydrodynamic instability in laminar flames. Part I. Derivation of basic equations, Acta Astronautica 4 (1977) 1177.
[20] H. Chaté and P. Manneville, Phase turbulence, in: Turbulence, a Tentative Dictionary eds. P. Tabeling and O. Cardoso, NATO ASI Series, Series B: Physics Vol. 341 (Plenum, Press, New York, 1994).
[21] B. Nicolaenko, B. Scheurer, and R. Temam, Attractors for the Kuramoto–Sivashinsky equations, Lectures in Applied Mathematics 23 (1986) 149.
[22] H. Sakaguchi, Breakdown of phase turbulence, Progr. Theoret. Phys. 84 (1990) 792.
[23] J. Krug and H. Spohn, Kinetic roughening of growing surfaces, in: Solids Far From Equilibrium ed. C. Godrèche (Cambridge University Press, Cambridge, 1991);
[24] M. Kardar, G. Parisi and Y.-C. Zhang, Dynamics of growing interfaces, Phys. Rev. Lett. 56 (1986) 889.

[25] L.-H. Tang, B.M. Forrest and D.E. Wolf, Kinetic surface roughening. Part II. Hypercube-stacking models, Phys. Rev. A 45 (1992) 7162.
[26] S.F. Edwards and D.R. Wilkinson, The surface statistics of a granular aggregate, Proc. Roy. Soc. London Ser. A 381 (1982) 17.
[27] Y.-C. Zhang, Non-universal roughening of kinetic self-affine interfaces, J. Phys. France 51 (1990) 2129; M.H. Jensen and I. Procaccia, Unusual exponents in interface roughening: The effects of pinning, J. Phys. II France 1 (1991) 1139.
[28] V. Yakhot, Large scale properties of unstable systems governed by the Kuramoto–Sivashinsky equation, Phys. Rev. A 24 (1981) 642.
[29] S. Zaleski, A stochastic model for the large scale dynamics of some fluctuating interfaces, Physica D 34 (1989) 427.
[30] K. Sneppen, J. Krug, M.H. Jensen, C. Jayaprakash and T. Bohr, Dynamic scaling and crossover analysis for the Kuramoto–Sivashinsky equation, Phys. Rev. A 46 (1992) 7351.
[31] F. Hayot, C. Jayaprakash and Ch. Josserand, Long-wavelength properties of the Kuramoto–Sivashinsky equation, Phys. Rev. E 47 (1993) 911.
[32] V.S. L'vov, V.V. Lebedev, M. Paton and I. Procaccia, Proof of scale invariant solutions in the Kardar–Parisi–Zhang and Kuramoto–Sivashinsky equations in $1+1$ dimensions: Analytical and numerical results, Nonlinearity 6 (1993) 25.
[33] C.C. Chow and T. Hwa, Defect-mediated stability: An effective hydrodynamic theory of spatiotemporal chaos, Physica D 84 (1995) 494.
[34] H. Chaté, in preparation.
[35] I. Procaccia, M.H. Jensen, V.S. L'vov, K. Sneppen and R. Zeitak, Surface roughening and the long-wavelength properties of the Kuramoto–Sivashinsky equation, Phys. Rev. A 46 (1992) 3220.
[36] V.S. L'vov and I. Procaccia, Comparison of the scale invariant solutions of the Kuramoto–Sivashinsky and Kardar–Parisi–Zhang equations in d dimensions, Phys. Rev. Lett. 69 (1992) 3543.
[37] C. Jayaprakash, F. Hayot and R. Pandit, Universal properties of the two-dimensional Kuramoto–Sivashinsky equation, Phys. Rev. Lett. 71 (1993) 12.
[38] V. L'vov and I. Procaccia, Comment on Universal properties of the two-dimensional Kuramoto–Sivashinsky equation, and reply by C. Jayaprakash, F. Hayot and R. Pandit, Phys. Rev. Lett. 72 (1994) 307, 308.
[39] G. Grinstein, C. Jayaprakash and R. Pandit, Conjectures about phase turbulence in the complex Ginzburg–Landau equation, Physica D 90 (1996) 96.
[40] L.-H. Tang and T. Natterman, Kinetic Surface Roughening. Part I. The Kardar–Parisi–Zhang equation in the weak coupling regime, Phys. Rev. A 45 (1992) 7156.